J Mater Sci: Mater Med (2008) 19:2761–2769
DOI 10.1007/s10856-008-3404-7

Evaluation of an injectable, photopolymerizable three-dimensional scaffold based on D,L-lactide and ε-caprolactone in a tibial goat model

Geert Vertenten · Lieven Vlaminck · Tomasz Gorski · Elke Schreurs · Wim Van Den Broeck · Luc Duchateau · Etienne Schacht · Frank Gasthuys

Received: 16 January 2007 / Accepted: 5 February 2008 / Published online: 29 February 2008

Abstract An in situ crosslinkable, biodegradable, methacrylate-encapped porous bone scaffold composed of D,L-lactide, ε-caprolactone, 1,6-hexanediol and poly(ortho-esters), in which crosslinkage is achieved by photoinitiators, was developed for bone tissue regeneration. Three different polymer mixtures (pure polymer and 30% bioactive glass or α-tricalcium phosphate added) were tested in a uni-cortical tibial defect model in eight goats. The polymers were randomly applicated in one of four (6.0 mm diameter) defects leaving a fourth defect unfilled. Biocompatibility and bone healing properties were evaluated by serial radiographies, histology and histomorphometry. The pure polymer clearly showed excellent biocompatibility and moderate osteoconductive properties. The addition of α-TCP increased the latter characteristics. This product offers potentials as a carrier for bone healing promoter substances.

G. Vertenten (✉) · L. Vlaminck · F. Gasthuys
Department of Surgery and Anaesthesiology of Domestic Animals, Faculty of Veterinary Medicine Ghent, Salisburylaan 133, Merelbeke 9820, Belgium
e-mail: geert.vertenten@ugent.be

L. Vlaminck
e-mail: lieven.vlaminck@ugent.be

F. Gasthuys
e-mail: frank.gasthuys@ugent.be

T. Gorski · E. Schacht
Polymer Material Research Group, Faculty of Sciences Ghent, Krijgslaan 281 (S4), Ghent 9000, Belgium
e-mail: etienne.schacht@ugent.be

E. Schreurs
Department of Medical Imaging of Domestic Animals, Faculty of Veterinary Medicine Ghent, Salisburylaan 133, Merelbeke 9820, Belgium
e-mail: elke.schreurs@ugent.be

W. Van Den Broeck
Department of Morphology, Faculty of Veterinary Medicine Ghent, Salisburylaan 133, Merelbeke 9820, Belgium
e-mail: wim.vandenbroeck@ugent.be

L. Duchateau
Department of Physiology and Biometry, Faculty of Veterinary Medicine Ghent, Salisburylaan 133, Merelbeke 9820, Belgium
e-mail: luc.duchateau@ugent.be

1 Introduction

Large bone defects in man and animals are a challenge for reconstructive surgery. Traditional techniques are based on the transplantation of homologous bone tissue [1–4]. However, the supply of adequate bone is often limited and the collection is painful with risk of haemorrhage, infection, nerve damage, cosmetic disability and loss of function [5].

Newer techniques involve the use of natural and synthetic bone grafts. The main recognised bone substitute groups are: calcium phosphates (bone-derived, synthetic ceramics, coralline hydroxyapatites, hydroxyapatite-composites, tricalcium phosphates), calcium carbonates (natural coral), calcium sulphate (plaster of Paris), glass and glass-ceramics, polymers, metals, bone and bone-derived materials (autograft, allograft, xenograft, demineralised bone matrix) and osteoinductive growth factors (BMPs and TGFβ-family). Most of the substitutes can be used for filler-reconstruction of moderate-sized (1–4 cm of diameter) cystic lesions in skeleton, but only a few can be used as a replacement for a weight bearing part of the

skeleton. The ultimate goal is to combine the strength of metals and polymers with the osteoconductivity, or preferably osteoinductivity of other types of materials resulting in an ideal bioactive composite implant with a suitable hardness, strength and modulus corresponding to the biomechanical properties of bone [6].

The increasing popularity of arthroscopic procedures in orthopaedics and the requirement to bridge large and irregular bone defects resulted in great interest in fixation materials that are injectable, in situ forming and biodegradable. Several injectable materials have been used as osteogenic bone substitutes. However, none has gained universal acceptance. The most commonly used injectable bone material polymethylmethacrylate is not biodegradable and polymerizes with production of high temperatures. If the polymerization reaction occurs outside the body, heat is not generated during implantation but the polymer often does not fit completely in irregular and large bone defects. Most composite polymers are not biodegradable [7]. Injectable scaffolds generally necessitate to solidify their constituent precursors or macromonomers into a three-dimensional matrix. Typical solidification mechanisms during the scaffold formation include: calcium phosphate setting, thermally or photochemically activated radical polymerization or crosslinking, chemical crosslinking, enzymatic crosslinking, thermal gelation, ionic gelation, ionic crosslinking, Michael-type addition reactions, and self-assembly mechanisms [8]. In situ formation of these scaffolds in the bone defect provides many advantages over ex vivo preparation and production of a correctly sized graft including improved contact between the scaffold and surrounding tissue [8].

The development of injectable biodegradable orthopaedic biomaterials which polymerize under controlled conditions can provide an alternative to current treatments for debilitating orthopaedic conditions [9]. This type of injectable material should be able to polymerize in situ in a relatively short period of time without negative effects on the surrounding tissue. It must be biocompatible, promote formation of new bone tissue, have appropriate viscosity before and efficient mechanical properties after setting, and can be sterilized [7]. Recently, tissue engineering offered potential solutions for functional and structural restoration of damaged or lost tissue. Tissue engineering of bone requires a suitable osteoconductive and inductive matrix [10–12], and additional sources of osteogenic cells.

A new in situ crosslinkable, biodegradable, methacrylate-encapped bone scaffold composed of D,L-lactide, ε-caprolactone, 1,6-hexanediol and poly(ortho-esters), in which cross-linkage is achieved by photo-initiators, was recently developed for bone tissue regeneration. By adding precise amounts of gelatine particles of selected size, a scaffold can be obtained with controlled porosity, pore size and pore connectivity. In addition, calcium phosphates, other osteoconductive materials or demineralised bone can be added to promote osteoconduction. The in vitro bioresorbable and osteoconductive properties of this new polymer have been described [13].

The objective of this study was to investigate biocompatibility of this bone substitute in a goat model and to evaluate its effect on bone regeneration in a uni-cortical tibial defect study.

2 Materials and methods

The study was approved by the Ethical Committee of the Faculty of Veterinary Medicine of the University of Ghent (EC 2004/86).

2.1 Preparation of scaffolds

Three different scaffolds were used in the study. Composite No. 1 was purely composed of poly-(D,L-lactide-co-ε-caprolactone) with 15 wt% 2-hydroxyethyl methacrylate polyester [13]. This basis was further mixed with 30% bioactive glass and 30% α-tricalcium phosphate (α-TCP) in composite No. 2 and 3, respectively. In order to create scaffolds with 70% porosity, an appropriate amount of gelatine particles (size of 250–355 μm) was added in all three of them.

All materials were sterilized by ethylene oxide (12 h, 37°C, 48 h degassing) and mixed under sterile conditions immediately before implantation.

2.2 Surgical procedure

Eight adult female goats with a mean age of 2.22 ± 0.55 years and a mean body weight of 53.2 ± 4.9 kg were used. The goats were housed in groups and had continuously access to food and water.

The goats were deprived of food for 48 h and received sodium ceftiofur (Excenel®, Pfizer Animal Health) (0.2 g IM) and flunixine (Finadyne®, Schering Plough Animal Health) (200 mg IM) 6 h before surgery. After sedation with xylazine (Xyl-M®, VMD) (0.2 mg/kg IM), anaesthesia was induced with midazolam (Dormicum®, Roche) and ketamine (Anesketin®, Eurovet NV) (respectively 0.011 mg/kg, 2.2 mg/kg IV) and maintained with isoflurane (IsoFlo®, Abbott) in oxygen using a routine monitoring protocol (ECG, pulsoximetry, capnography, direct blood pressure and arterial blood gasses). Ringer's lactate solution (5 ml/kg/h) was administered during the anaesthetic period.

The animals were placed in dorsal recumbency with both hindlegs separately suspended. After surgical

preparation, a 10 cm longitudinal skin and periosteal incision was made midway and medial to each tibia. The periosteum was elevated and four holes (6.0 mm diameter) were drilled in the medial diaphyseal cortex of the tibia using a trephine burr (3I®, Implant Innovations). Sterile physiologic saline was used for cooling during burring. The centre of the most proximal defect was drilled at 2.25 cm proximal to the predetermined midpoint of the tibia. Each additional hole was drilled 1.5 cm more distally using a sterile plastic template. Hemostasis was provided by use of epinephrine soaked gauzes pushed in the defects prior to application of the bone substitute. In each leg, the three composites were randomly assigned to a hole whereas the fourth hole was left empty to serve as a control. Each composite was firstly placed on the borders and bottom of the defect and photopolymerized for 40 s (500 mW/cm^2 blue light, 3M Unitek Visible Light Curing Unit™). After setting, the remaining defect was further filled with a second layer of additional composite that was also photopolymerized prior to wound closure, The surgical incision was closed in three layers using continuous suture patterns and resorbable sutures. Postoperatively, the animals received sodium ceftiofur for 7 days (0.2 g IM) and flunixine meglumine for 3 days (200 mg IM). Two goats were euthanized 4 weeks and two other goats 8 weeks after surgery. One goat was further euthanized at 12, 18, 24 and 36 weeks after surgery.

2.3 Clinical and radiographic follow-up

During the study period, goats were daily evaluated for healing of the surgical site and development of complications related to the surgical intervention.

Immediately following surgery, cranio-caudal and latero-medial radiographic projections of each tibia were taken. Both digital as well as conventional radiographs were obtained. At 4 weeks intervals, bone healing was further radiographically evaluated up to 18 weeks postoperatively. A final radiographic evaluation was done in one goat at 24 and at 36 weeks after surgery in another animal.

The conventional radiographs were blindly evaluated for defect density, periosteal reaction and soft tissue reaction using the criteria of Dorea et al. [14] by two investigators (see Table 1).

Digital radiographs were used to measure grey scale densities at the level of the bone defects (Image J 1.34s).

2.4 Histological evaluation

After euthanasia, all soft tissue surrounding both tibias was removed. The tibial bones were split longitudinaly and the bone marrow was removed. Each defect site was separately isolated and fixed in formol 10% for 12 h. The samples were rinced with tap water and dehydrated at 4°C using an ethanol gradient (48 h in 50, 75 and 96% and 72 h in 100% ethanol). Afterwards samples were defatted in xylene for 48 h at 4°C and embedded in destabilised Technovit 9100 New® (Heraeus Kulzer) (polymerization for 24 h at 0°C). Four µm sections were cut with a microtome (SM2500, Leica Microsystems), stretched with 70% ethanol on a slide and dried for 12 h at 60°C.

The sections were stained with haematoxylin & eosin, Von Kossa and Toluidineblue stain. All samples were blindly evaluated under the microscope by the same investigator. They were evaluated for the tissue type, presence of residual graft material within the defect, the quality of bone healing and the presence of inflammatory reactions.

Histomorphometric analysis (AnalySIS) was performed on the Von Kossa stained sections obtained until 12 weeks after surgery using a 4× magnification (Olympus BX61 microscope). The volume of Von Kossa positive (black-brown), Von Kossa negative (violet) and colourless stained material were measured and expressed as a percentage of the total defect area.

Table 1 Scores for defect density, periosteal reaction and callus formation and soft tissue reaction [14]

Density		Size		Distribution		Soft tissue	
0	Radiolucent	0	None	0	None	0	No soft tissue reaction
−1	More radiolucent	1	Small	1	Regular and in the defect site	1	Moderate soft tissue reaction
1	Radiopaque	2	Moderate	2	Irregular but in the defects site	2	Severe soft tissue reaction
2	Mildly increased radiopacity	3	Abundant	3	Regular but out of the defect site		
3	Moderately increased radiopacity	4	Exaggerated	4	Irregular and out of the defect site		
4	Extensively increased radiopacity						

Density = density of the defect

Size = periosteal reaction and callus formation around each defect graded by size

Distribution = periosteal reaction and callus formation around each defect graded by distribution

Soft tissue = soft tissue reaction around the defects

2.5 Statistical analysis

The conventional radiograph scores (average of the two investigators) were compared between the three composites and the control defect by the Friedman test with tibia and time as block factor at the 5% global significance level. The four composites were pairwise compared by the stratified Wilcoxon rank sum test using Bonferroni's multiple comparisons adjustment technique.

The digital radiograph density assessments were analysed by a mixed model with tibia as random effect and composite, time, position and the interaction between composite and time as categorical fixed effects at the 5% global significance level.

Histological bone healing assessments were analysed by a mixed model with tibia as random effect and composite, time and the interaction between composite and time as categorical fixed effects at the 5% global significance level.

Pairwise comparisons in the mixed model were based on Bonferroni's multiple comparisons adjustment technique.

3 Results

Profuse bleeding was encountered during the creation of 25 uni-cortical bone defects which could be stopped by epinephrine soaked gauzes providing an acceptable hemostasis. All of the graft materials were easily implanted into the tibial defects and were considered stable prior to wound closure. None of the goats showed signs of pain or lameness during the study period. Except for discrete subcutaneous fluid accumulation in five animals at 4 weeks after surgery no other clinically visible adverse tissue reactions were observed.

3.1 Conventional radiographs

A significant difference between the composites was found for the density of each defect over time ($P < 0.0001$), with significant pairwise comparisons between the control and composite No. 1 ($P = 0.0002$) and between composite No. 1 and No. 3 ($P = 0.0008$) (see Fig. 1). The size of the periostal reaction and callus formation around each defect ($P = 0.0018$) differed significantly between the composites, with significant pairwise comparisons between the control and composite No. 1 ($P = 0.0007$) and between composite No. 1 and No. 3 ($P = 0.0046$) (see Fig. 2). No significant differences were found between the composites with respect to the distribution of the periosteal reaction and callus formation ($P = 0.17$) and the soft tissue reaction ($P = 0.179$) (see Figs. 3 and 4).

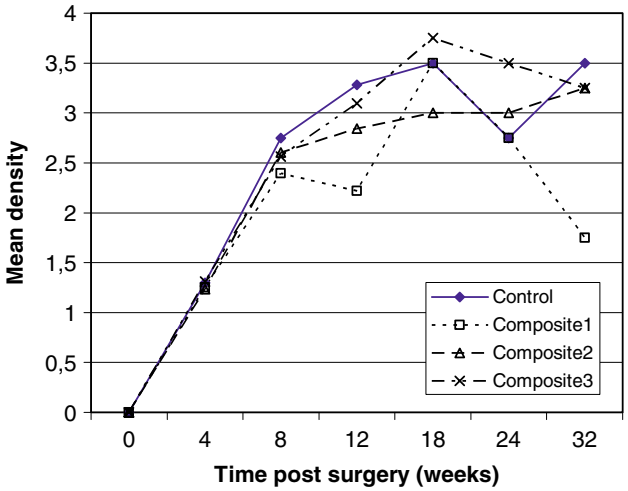

Fig. 1 Evolution of the mean densities of unicortical tibial defects treated with different composites based on serial conventional radiographic evaluation in eight goats

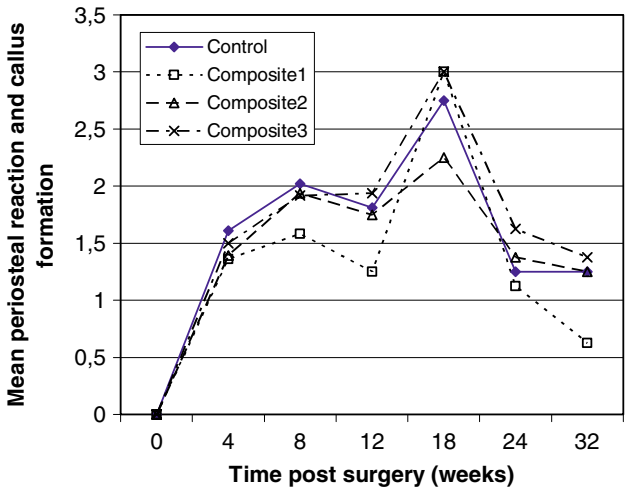

Fig. 2 Evolution of the mean periosteal reaction and callus formation around unicortical tibial defects treated with different composites based on serial conventional radiographic evaluation in eight goats

3.2 Digital radiographs

The mean density of the control defect and the defects with composites No. 1, No. 2 and No. 3 were respectively 79.5 ± 2.9, 76.0 ± 2.9, 77.6 ± 2.9 and 77.9 ± 2.9. No significant differences were found between the composites ($P = 0.64$), nor was there a significant interaction between composite and time ($P = 0.93$). Densities however differed significantly between radiographic projections ($P < 0.0001$). An overall mean density of 89.68 was calculated on latero-medial projections compared to 65.83 on cranio-caudal projections.

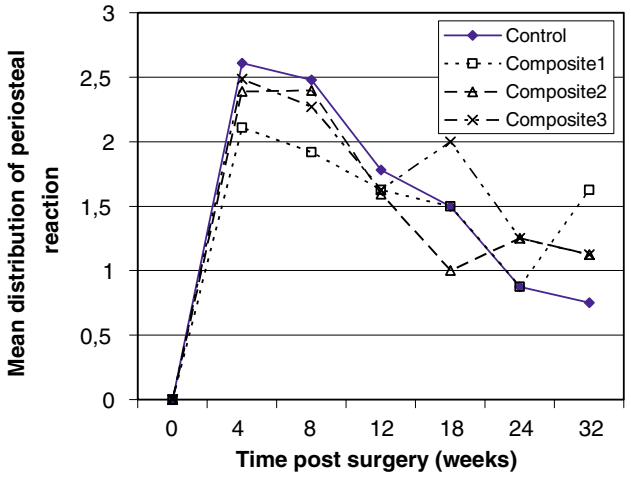

Fig. 3 Evolution of the mean distribution of periosteal reaction around tibial defects treated with different composites based on serial conventional radiographic evaluation in eight goats

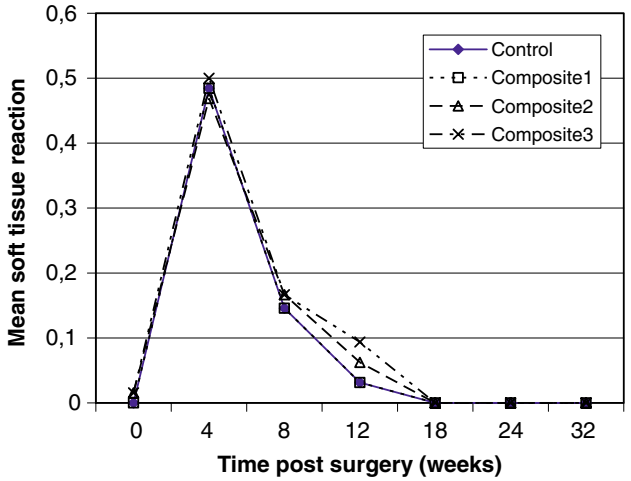

Fig. 4 Evolution of the mean soft tissue reaction around tibial defects treated with different composites based on serial conventional radiographic evaluation in eight goats

3.3 Histological evaluation

New bone formation was most pronounced in the control defects causing bridging of the defect by bone tissue as soon as 8 weeks after surgery (see Fig. 5). Independent of the type of composite used, the new bone formation was most pronounced at the periosteal and endosteal sides of the defects (see Fig. 6) which specifically resulted in the development of pronounced callus tissue on the periosteal side (see Fig. 7).

All composite treated defects were filled with a mixture of composite and both fibrous and bone tissue. Fibrous tissue was localised in the periphery and in the centre of the different composite materials. No bone precursors such as cartilage were observed. There was a slight ingrowth of

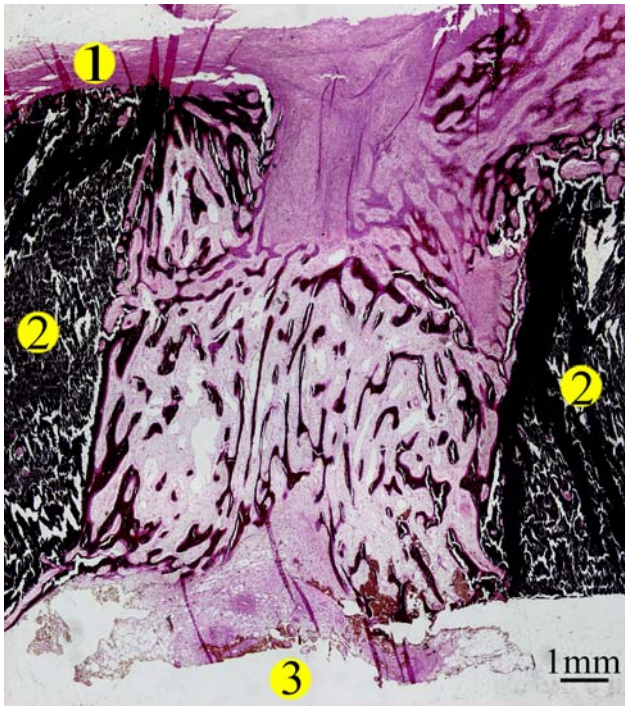

Fig. 5 Photomicrograph of a tibial control defect 8 weeks postoperative in a goat. A bridge of trabecular primary bone covers more than 50% of the original cortical defect. (1: periost; 2: normal corticalis surrounding defect; 3: medulla) (Von Kossa)

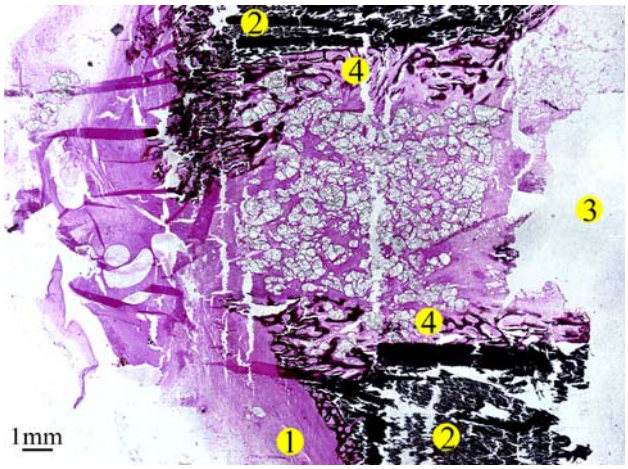

Fig. 6 Photomicrograph of a tibial defect treated with composite No. 3, 8 weeks postoperatively. The new bone formation is most pronounced at the periosteal and endosteal side of the defect. There is a slight ingrowth of bone at the periphery of the composite material (4) (1: periost; 2: normal cortex surrounding the defect; 3: medulla) (Von Kossa)

bone at the periphery of the composite materials visible (see Figs. 6 and 7). The quantitiy of composite material gradually decreased over time to completely disappear no sooner than 32 weeks after surgery (see Fig. 8). None of the defects showed signs of inflammatory or immunologic reactions.

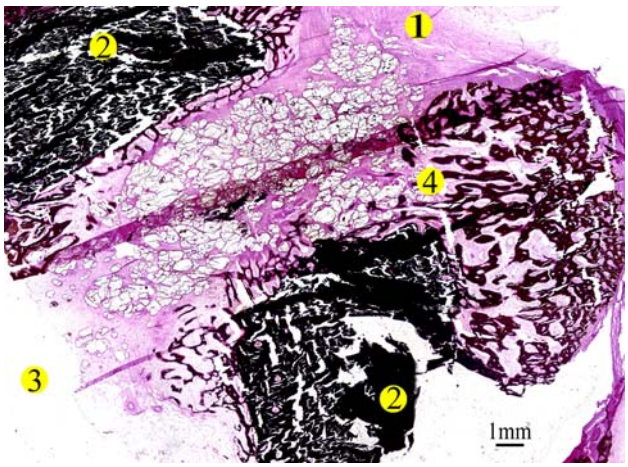

Fig. 7 Photomicrograph of a tibial defect treated with composite No. 2, 8 weeks postoperatively. A big bony callus is visible at the periosteal side of the defect. There is a slight ingrowth of bone at the periphery of the composite material (4) (1: periost; 2: normal cortex surrounding the defect; 3: medulla) (Von Kossa)

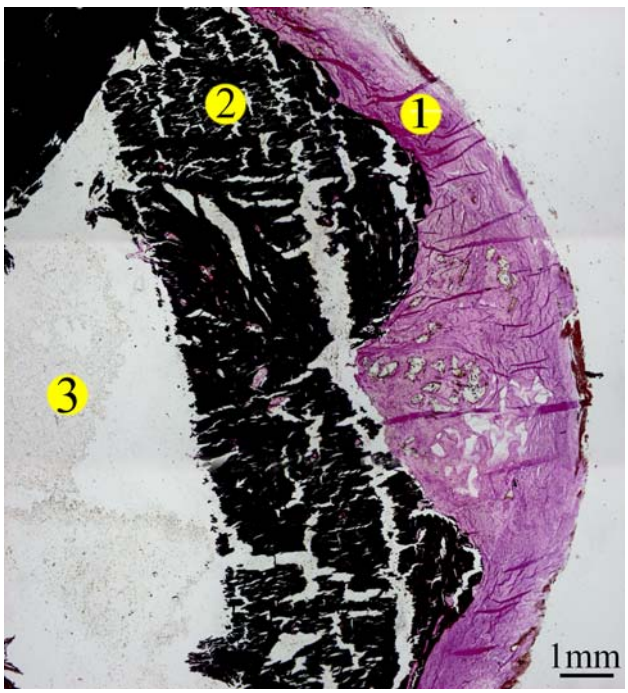

Fig. 8 Photomicrograph of a tibial defect treated with composite No. 2, 32 weeks postoperatively. Almost no composite left anymore. (1: periost; 2: normal cortex surrounding the defect; 3: medulla) (Von Kossa)

3.4 Histomorphometry (see Fig. 9)

The percentages of Von Kossa positive staining were significantly ($P = 0.0016$) influenced by the type of material used. Control defects contained significantly more Von Kossa positive material (mean 31.1% ± 4.4) compared to composites No. 1 ($P = 0.0012$) and 2 ($P = 0.0211$) (mean values of 13.4% ± 4.4 and 18.2% ± 4.4, respectively). No differences were found between control defects and defects containing composite No. 3 (23.9% ± 4.4, $P = 0.3096$), nor between the three composites.

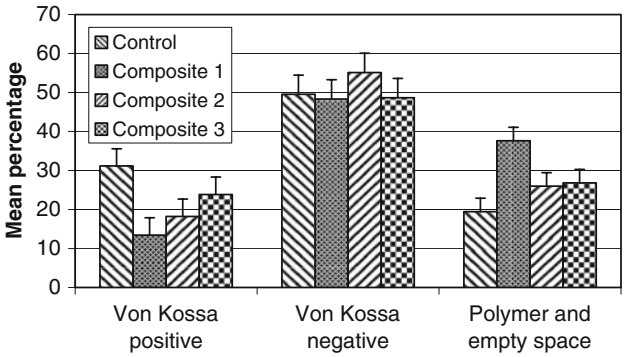

Fig. 9 Mean percentage (+standard deviation) of each tibial defect for Von Kossa positive, Von Kossa negative and empty space (only for goats that lived no longer then 12 weeks post-surgery)

The percentages of Von Kossa negative staining did not differ between the defects ($P = 0.366$). The mean percentages of control defects and defects filled with composites No. 1, 2 and 3 were 49.5% ± 4.9, 48.3% ± 5.0, 55.1% ± 5.0 and 48.7% ± 5.0, respectively.

Significant differences were found between the four groups ($P = 0.0036$) when evaluating the percentages of the colourless material. Empty defects (19.44% ± 3.4) contained significantly ($P = 0.002$) less colourless material compared to defects filled with composite No. 1 (37.6% ± 3.5). The other composites did not differ significantly (mean of composite No. 2: 25.99% ± 3.5; mean of composite No. 3: 26.82% ± 3.5).

4 Discussion

A new in situ crosslinkable, biodegradable, methacrylate-encapped bone scaffold composed of D,L-lactide, ε-caprolactone, 1,6-hexanediol as well as poly(ortho-esters) was recently developed for bone tissue regeneration. Solidification is done by photopolymerization, a commonly used technique in dental restorative procedures [15]. Photopolymerization has several advantages over conventional polymerization techniques including spatial and temporal control over polymerization, fast curing rates (less than a second to a few minutes) at room or physiological temperature, and minimal heat production [16]. Gelatine particles were included in the polymer to create porous scaffolds facilitating tissue ingrowth and vascularization. These characteristics have been demonstrated by Declercq et al. [13] who compared the osteoconductivity of scaffolds with different apparent porosities (50, 60 and 70) and different porosigens (gelatine, sodium chloride, and sugar) by

scanning electron microscopy and histological analysis. The same authors further proved the bioresorbable and osteoconductive properties of the polymer in an in vitro setting using osteoblast cell cultures. In the present study these same properties were tested in an in vivo setting using the pure scaffold and combinations with bone substitutes (α-TCP and bioactive glass) that have proven their influence on bone healing in other studies [17, 18].

Goats were used in the present study because of their easiness in handling and housing and their frequent use as experimental animals in orthopaedic and bone substitute research [19–24]. The use of a critical sized defect model, as has been described in small laboratory animals [25–33] as well as sheep [34–38], was considered too invasive in the current stadium of the ongoing research. The use of uni-cortical cylindrical defects has been reported for experimental work on bone substitutes and bone healing [14, 39–42]. The medial diaphyseal cortex of the tibia was preferred for creation of cortical defects because it can be easily approached for surgical intervention with minimal dissection. Although none of the animals in the present study developed important postoperative complications related to the surgical intervention, specific care should be taken to prevent excessive weight-bearing and possible tibial fracture as has been observed in comparable experiments using sheep (Vertenten, personal communication).

During the surgical interventions profuse bleeding from the bone marrow hindered the static positioning of the bone substitutes before setting as this experimental substance did not stick to bone in humid environments. This problem was easily overcome by using epinephrine soaked gauzes to provide hemostasis. To avoid inadvertent application of the composite in the medullary cavity, photopolymerisation was performed in two steps. This further assured complete polymerisation of the entire volume of applicated bone substitute.

Bone healing is routinely analysed by histomorphological, histometrical and immunohistochemical techniques as means of assessing the differentiation status of bone deposition and growth. Currently, few embedding resins exist for which both morphological and immunohistochemical analyses can be performed on mineralised tissue. Paraffin, the standard embedding medium for bone enzyme and immunohistochemistry is only suitable for use with demineralised tissue that often shows badly preserved trabecular structure [43]. Methyl methacrylate (MMA) which is the first choice embedding resin for histological examination of undecalcified bone precludes immunohistochemal analysis because of its exothermic polymerisation reaction destroying both enzyme activity and tissue antigenicity. Technovit 9100 New® is a low temperature MMA embedding resin that has been reported to significantly improve tissue antigenicity preservation as it allows polymerisation at −20°C [43]. Therefore, this resin was chosen to allow optimal immunohistochemical analysis of the obtained bone samples in this study. A supplementary difficulty of MMA embedded tissue is the difficulty to make thin sections. Sections are usually cut between 50 μm and 500 μm [44–47] and sometimes grinded to 10–40 μm [48–50]. With the SM2500 microtome undecalcified sections of 4 μm could be made. Those thin sections were very fragile, so gentle manipulation was needed. Nevertheless thin sections make it easier to evaluate the tissues as there is less superposition of several tissue layers. As grinding of the section is unnecessary, more sections can be made and tissue can be evaluated at more levels and by more different stainings.

Bone healing was evaluated by both conventional as well as digital radiographs on fixed time intervals. The conventional radiographs were interpreted blindly by two persons in a similar way as Dorea et al. [14] using categorical variables what increases the likelihood of finding significant differences in contrast to the use of continual variables as were produced in density measurements on digital radiographies. The highest overall mean density was observed in the control defect followed by composites No. 3, No. 2 and No. 1, respectively. The observed differences in densities between the different projections can be explained by the superposition of the lateral cortex on the latero-medial projections causing a larger density then on cranio-caudal projections.

The observed density differences between composites and the more pronounced periosteal reaction of composite No. 3 based on conventional radiographs suggest an advantage of adding α-TCP to the polymer. The absence of distribution differences of the periosteal reaction, callus formation and soft tissue reactions might indicate a comparable immunologic reaction to the different bone substitutes.

The present study clearly illustrated the excellent biocompatibility of the different polymer mixtures illustrated by the absence of inflammatory signs on histological examination.

Von Kossa positive material corresponds with phosphate and carbonate, the anions that bind calcium in tissues. On the bone sections in the present study, this corresponded with mineralized bone as well as the presence of bioactive glass and α-TCP particles. Von Kossa negative material mainly represents the presence of fibrous tissue whereas colourless zones indicated the presence of the pure polymer as well as artifacts. No histomorphometric evaluation of bone samples obtained after more than 12 weeks postoperatively was performed as it was impossible to identify the original defects in these cases because of pronounced periosteal reactions. Histomorphometrical evaluation demonstrated slower bone healing and remodelling in the

presence of composites in comparison with control defects. This was not a surprising result as tissue ingrowth and gradual degradation of bone substitutes is more time consuming than the rate of new bone formation in the absence of foreign material. Polymer degradation was not optimal as was illustrated by the formation of fibrous tissue in and around the composite material. The polymer did not induce fibrous tissue formation as no differences in terms of percentage were seen between control and treated defects. The lack of new bone formation in the centre of the different composite treated defects reflects a lack of osteoconductive properties despite the porous architecture of the used polymers. This problem might be improved by the addition of cellular bone precursors or osteoconductive inducing substances.

5 Conclusion

This study demonstrated the excellent biocompatible results of the examined polymer poly(D,L-lactide-co-ε-caprolactone) + 15 wt% 2-hydroxyethyl methacrylate but was unable to show osteoconductive properties after application in non critical sized defects in goats tibias . The addition of α-TCP had a positive influence on bone healing. Further biochemical enhancement is needed to optimize porous architecture and degradation properties. It can be concluded that this material offers potentials as a carrier for other bone healing promoting substances.

Acknowledgments The authors thank Cindy De Baere, Bart De Pauw, Liliana Standaert and Lobke De Bels for technical assistance.

References

1. T.J. Slooff, P. Buma, B.W. Schreurs, J.W. Schimmel, R. Huiskes, J. Gardeniers, Clin. Orthop. Relat. Res. **324**, 108 (1996)
2. K.M. Malloy, A.S. Hilibrand, Clin. Orthop. Relat. Res. **394**, 27 (2002)
3. W.G. Paprosky, E.L. Martin, Am. J. Orthop. **31**, 81 (2002)
4. A.E. Gross, H. Blackley, P. Wong, K. Saleh, I. Woodgate, Instr. Course Lect. **51**, 103 (2002)
5. C. Damien, R. Parsons, J. Appl. Biomat. **2**, 187 (1991)
6. A.J. Aho, J.T. Heikkila, in *Clinical Applications of Bone Allografts and Substitutes—Biology and Clinical Applications* (World Scientific Publishing Co, Singapore, 2005). p. 139
7. J.S. Temenoff, A.G. Mikos, Biomaterials **21**, 2405 (2000)
8. Q. Hou, P.A. de Bank, K.M. Shakesheff, J. Mater. Chem. **14**, 1915 (2004)
9. J.A. Burdick, K.S. Anseth, Biomaterials **23**, 4315 (2003)
10. D.W. Hutmacher, Biomaterials **21**, 2529 (2000)
11. L.L. Hench, J.M. Polak, Science **295**, 1014 (2002)
12. F.R. Rose, R.O. Oreffo, Biochem. Biophys. Res. Commun. **292**, 1 (2002)
13. H.A. Declercq, T.L. Gorski, S.P. Tielens, E.H. Schacht, M.J. Cornelissen, Biomacromolecules **6**, 157 (2005)
14. H.C. Dorea, R.M. McLaughlin, H.D. Cantwell, R. Read, L. Armbrust, R. Pool, J.K. Roush, C. Boyle, Vet. Comp. Orthop. Traumatol. **18**, 157 (2005)
15. Z. Tarle, A. Meniga, M. Ristic, J. Sutalo, G. Pichler, C.L. Davidson, J. Oral Rehabil. **25**, 436 (1998)
16. K. Nguygen, J.L. West, Biomaterials **23**, 4307 (2002)
17. P. Virolainen, J. Heikkila, A. Yli-Urpo, E. Vuori, H.T. Aro, J. Biomed. Mater. Res. **35**, 9 (1997)
18. J.E. Fleming, C.N. Cornell, G.F. Muschler, Orthop. Clin. N. Am. **31**, 357 (2000)
19. S. Van Der Donk, P. Buma, P. Aspenberg, B.W. Schreurs, Comp. Med. **51**, 336 (2001)
20. R.P. Meinig, Injury **33**, 58 (2002)
21. P. Buma, W. Schreurs, N. Verdonschot, Biomaterials **25**, 1487 (2004)
22. K.R. Dai, X.L. Xu, T.T. Tang, Z.A. Zhu, C.F. Yu, J.R. Lou, X.L. Zhang, Calcif. Tissue Int. **77**, 55 (2005)
23. X.L. Xu, T.T. Tang, K.R. Dai, Z.A. Zhu, X.E. Guo, C.F. Yu, J.R. Lou, Acta Orthop. **76**, 637 (2005)
24. X. Li, Q. Feng, X. Liu, W. Dong, F. Cui, Biomaterials **27**, 1917 (2006)
25. J.W. Frame, J. Oral Surg. **38**, 176 (1980)
26. S.G. Hopp, L.E. Dahners, J.A. Gilbert, J Orthop. Res. **7**, 579 (1989)
27. J.O. Hollinger, J.C. Kleinschmidt, J. Craniofac. Surg. **1**, 60 (1990)
28. H.D. Zegsula, D.C. Buck, J. Brekke, J.M. Wozney, J.O. Hollinger, J. Bone Joint Surg. Am. **79**, 1778 (1997)
29. M.A. Shermak, L. Wong, N. Inoue, T. Nicol, J. Craniofac. Surg. **11**, 224 (2000)
30. E.L. Liljensten, A.G. Attaelmanan, C. Larsson, H. Ljusberg-Wahren, N. Danielsen, J.M. Hirsch, P. Thomson, Clin. Implant Dent. Relat. Res. **2**, 50 (2000)
31. K.U. Lewandrowski, J.D. Gresser, S. Bondre, A.E. Silva, D.L. Wise, D.J. Trantolo, J. Biomater. Sci. Polym. Ed. **11**, 879 (2000)
32. P.B. Saadeh, R.K. Khosla, B.J. Mehrara, D.S. Steinbrech, S.A. Mccormic, D.P. Devore, M.T. Longaker, J. Craniofac. Surg. **12**, 573 (2001)
33. S. Stal, K. Tjelmeland, J. Hicks, N. Bhatia, B. Eppley, L. Hollier, J. Craniofac. Surg. **12**, 41 (2001)
34. C.A. Kirker-Head, T.N. Gerhart, R. Armstrong, S.H. Schelling, L.A. Carmel, Clin. Orthop. Relat. Res. **349**, 205 (1998)
35. O. Shang, Z. Wang, W. Liu, Y. Shi, L. Cui, Y. Cao, J. Craniofac. Surg. **12**, 586 (2001)
36. K.U. Lewandrowski, J.D. Gresser, S. Bondre, A.E. Silva, D.L. Wise, D.J. Trantolo, J. Biomater. Sci. Polym. Ed. **11**, 197 (2000)
37. K.U. Lewandrowski, J.D. Gresser, S. Bondre, A.E. Silva, D.L. Wise, D.J. Trantolo, J. Biomater. Sci. Polym. Ed. **11**, 209 (2000)
38. M.A.K. Liebschner, Biomaterials **25**, 1697 (2004)
39. D. Griffon Jr., R. Mclaughlin, J. Hoskinson, Vet. Comp. Orthop. Traumatol. **9**, 22 (1996)
40. S.R. Macneill, C.M. Cobb, J.W. Rapley, A.G. Glaros, P. Spencer, J. Clin. Periodontol. **26**, 239 (1999)
41. M. Dalkyz, A. Ozcan, M. Yapar, N. Gokay, N. Yuncu, Implant. Dent. **9**, 226 (2000)
42. R.P. Meinig, Injury **33**, 683 (2002)
43. R. Yang, C.M. Davies, C.W. Archer, R.G. Richards, Eur. Cell. Mater. **6**, 57 (2003)
44. E. Jallot, J.L. Irigaray, G. Weber, P. Frayssinet, Surf. Interface Anal. **27**, 648 (1999)
45. Z. Gugala, S. Gogolewski, J. Orthop. Trauma. **3**, 187 (1999)
46. P. Chistoline, I. Ruspantini, P. Bianco, A. Corsi, R. Cancedda, R. Quarto, J. Mater. Sci. Mater. Med **10**, 739 (1999)
47. S. Kessler, U. Mayr-Wohlfart, A. Ignatius, W. Puhl, L. Claes, K.P. Gunter, Arch. Orthop. Trauma Surg. **121**, 472 (2001)

48. M. Lamghari, H. Huet, A. Laurent, S. Berland, E. Lopez, Biomaterials **20**, 2107 (1999)
49. G. Cunin, H. Boissonnet, H. Petite, C. Blanchat, G. Guillemin, Spine **9**, 1070 (2000)
50. T.J. Blokhuis, B.W. Wippermann, F.C. Den Boer, A. Van Lingen, P. Patka, F.C. Bakker, H.J.T.M. Haarman, J. Biomed. Mater. Res. **51**, 369 (2000)